

# Self-powered triboelectric aptasensor for label-free highly specific thrombin detection



Yun Kyung Jung<sup>a,b</sup>, Kyeong Nam Kim<sup>c</sup>, Jeong Min Baik<sup>c,\*</sup>, Byeong-Su Kim<sup>b,d,\*\*</sup>

<sup>a</sup> School of Biomedical Engineering, Inje University, Gimhae, Gyeongnam 50834, Republic of Korea

<sup>b</sup> Department of Energy Engineering, Ulsan National Institute of Science and Technology (UNIST), Ulsan 44919, Republic of Korea

<sup>c</sup> School of Materials Science and Engineering, KIST-UNIST-Ulsan Center for Convergent Materials, Ulsan National Institute of Science and Technology (UNIST), Ulsan 44919, Republic of Korea

<sup>d</sup> Department of Chemistry, Ulsan National Institute of Science and Technology (UNIST), Ulsan 44919, Republic of Korea

## ARTICLE INFO

### Keywords:

Triboelectric

Biosensor

Gold nanoparticle

Thrombin

Aptamer

## ABSTRACT

An aptamer-based triboelectric biosensor is developed for a highly specific, label-free and self-powered detection of thrombin. For the first time, intermolecular recognition interactions are used to develop a selective nanosensor based on triboelectric effect. Positively charged Au nanoparticles (Au NPs<sup>+</sup>) with large difference in triboelectric polarity and work function are assembled onto Al film to increase the electrical output of triboelectric nanogenerators (TENG). Modification of anti-thrombin aptamers on the Au NPs<sup>+</sup>-assembled TENG affords the triboelectric nanosensor highly selective toward thrombin, even in clinical samples because of specific binding affinity between aptamers and thrombin unlike random DNA-modified TENGs with undetectable response. A 0.41 nM limit of detection is achieved, which is directly demonstrated by the number of commercial LED lights without any supporting equipment such as power source and electrometer. Our study demonstrates an innovative and unique approach toward the self-powered and label-free detection of thrombin for rapid and simple in-field analysis.

## 1. Introduction

Detection of disease-related proteins holds significant applications in clinical diagnosis [1–3]. Thrombin, a serine protease involved in the coagulant cascade has great importance in physiological and pathological processes [4,5], such as regulation of tumour growth, metastasis, and angiogenesis [6]. The concentration of thrombin in blood depends on the physical condition of the subject. Thrombin can be almost absent in the blood of healthy subjects, but it can vary from low nanomolar to micromolar concentrations during the coagulation process [7]. Taking advantage of high specificity of intermolecular recognition reactions between thrombin and thrombin-specific ligands such as antibody or aptamer, significant efforts have been made to develop biosensors to directly detect thrombin.

Among various biological recognition elements which determine the degree of selectivity of the biosensor, nucleic acid-based aptamers have been recognized as very promising bioreceptors because of their outstanding selectivity, sensitivity, and stability [8]. Notably, thrombin binding to its aptamer is the most commonly and intensively used model system to demonstrate aptamer-based affinity assays in the

clinical area [9–17]. Optical and electrochemical approaches have primarily been applied to detect the thrombin [1–3,10–17]. For example, colorimetry and fluorometry are the most widely used due to their convenience, high sensitivity, and application to point-of-care testing [1–3,11–17]. However, there are still significant challenges including complicated and time-consuming probe-labelling steps, high background noise, and difficulties in inferring accurate and quantitative results from the collected optical signals. In contrast, electrochemical approaches are advantageous in label-free and quantitative measurement capability as well as being practicable for in-field lab-on-a-chip devices, yet they have some limitations related to relatively low detection sensitivity, electrode fouling, electrochemical stability of reagents, side electrochemical reactions, and most critically, the requirement for an external power supply [2,3,10,12].

Recently, the concept of self-powered sensors based on the triboelectric nanogenerator (TENG), which converts mechanical energy from the environment into electricity, has received considerable attention because no battery is needed to power the device [18–23]. Considering the operational mechanism of self-powered device, the electric output signal can be critically determined by molecules

\* Corresponding author.

\*\* Corresponding author at: Department of Energy Engineering, Ulsan National Institute of Science and Technology (UNIST), Ulsan 44919, Republic of Korea.  
E-mail addresses: [jbaik@unist.ac.kr](mailto:jbaik@unist.ac.kr) (J.M. Baik), [bskim19@unist.ac.kr](mailto:bskim19@unist.ac.kr) (B.-S. Kim).

adsorbed on an electrically active surface. Although Wang and co-workers have reported the early examples of sensing by TENG for mercury ions and glucose [18,19], their system was focused on the marker specific to mercury ions or the TENG was used as a power source for the sensor. There has been no report on the use of selective binding events which have specific energy states in this type of sensors to date. Thus, specific, label-free and self-powered methods are highly desirable for rapid and simple in-field analysis.

Herein, we describe the development of an aptamer-based triboelectric biosensor for the highly specific, label-free and self-powered detection of thrombin. For the first time, specific aptamer-protein interactions are used to develop a fully integrated, stand-alone and self-powered nanosensor. With respect to previous works in the field, our approach is unique in a number of attributes. First, to maximize the charge density on both surfaces, the materials with the largest difference in triboelectric polarity [24] and work function [24] are chosen. In that sense, positively charged Au nanoparticles (Au NPs<sup>+</sup>) with large surface area [25] were assembled onto the Al film to improve the performance of the TENG [26]. These assembled Au NPs<sup>+</sup> not only act as steady gaps between the two plates at the strain-free condition, but also increase the electrical output of the TENG by enlarging the contact area of the two plates. Second, through modification of thiol-modified anti-thrombin aptamers on the assembled Au NPs<sup>+</sup>, the nanogenerator became a highly selective nanosensor toward thrombin detection because of the strong binding affinity between them. On the basis of this unique structure, the output voltage and current of the Au NPs<sup>+</sup>-assembled triboelectric nanosensor significantly decreased after decoration with negatively charged aptamers. Under optimum conditions, this aptamer-modified TENG sensor showed the enhanced electrical signals only after incubation with thrombin, with a detection limit of 0.41 nM. The random DNA-modified TENG did not show any response to thrombin. Third, the electricity generated by the interactions with thrombin directly lit up commercial green LEDs, which showed great potential as a simple detection systems as well as facilitating label-free sensing without complex labelling of expensive dyes. Our study demonstrates a unique advanced approach toward the self-powered detection of thrombin for rapid and simple in-field analysis compared to the widely used colorimetric or fluorometric methods (Table S1).

## 2. Experimental section

### 2.1. Materials

Thiol-modified oxidized (S-S) TASSET aptamer sequences (5'-AGT CCG TGG TAG GGC AGG TTG GGG TGA CT-3') and random DNAs (5'-CGT TAC AGT TGG GTA ACG GG-3') were synthesized and purified by Integrated DNA Technologies (Coralville, IA, USA). Other proteins and chemicals including thrombin from human plasma, streptavidin (Str), lysozyme (Lyso), HEPES, and MgCl<sub>2</sub> were purchased from Sigma-Aldrich, Inc. (St. Louis, MO, USA) and used without further purification. Sample stock solutions were prepared by directly dissolving the proteins in HEPES buffer (1.0 mM HEPES, 1.0 mM MgCl<sub>2</sub>, pH 7.26) and stored in a refrigerator at -20 °C. Polydimethylsiloxane (PDMS, Sylgard 184, Dow Corning) were used for the fabrication of TENG. The base monomer (Sylgard 184A) and curing agent (Sylgard 184B) were mixed in a mass ratio of 10:1, followed by vacuum drying to degas the PDMS mixture. After 30 min, 1.0 mL of mixture was coated onto the silicon wafer, and allowed to solidify into an amorphous free-standing film by heating on an oven at 90 °C for 5 min.

### 2.2. Fabrication of TENGs

An aqueous solution of 0.40 mL of 4-(dimethylamino)pyridine (DMAP)-Au NPs (Au NP<sup>+</sup>) [26] and carboxylic acid-modified Au NPs (Au NP<sup>-</sup>) [27–30] (conc. of 60 mg/L) was casted on Al bottom electrode (1 cm×1 cm) and dried for 2 h at room temperature. One hundred μm-thick pure PDMS film was attached on the Al top electrode by the double sided polyimide tape. A triboelectric nanogenerator was prepared by stacking two pieces of the structures and mechanically triggered by a linear motor after optimizing the conditions for impact force and frequency (Fig. S1). As the input force and the frequency increase, the output current of the Au NP<sup>+</sup>-assembled TENG increases and reaches around 35 μA in both cases. A compressive force of 50 N and a frequency of 10 Hz were employed in this study to generate the high and reliable electrical signals by the TENG. The long-term stability of the Au NP<sup>+</sup>-assembled TENG was also evaluated by using a pushing tester for 24 h. As shown in Fig. S2, consistent output voltage of the TENG was maintained, demonstrating the successful integration of Au NPs onto the Al film substrate and its stability during the operation of

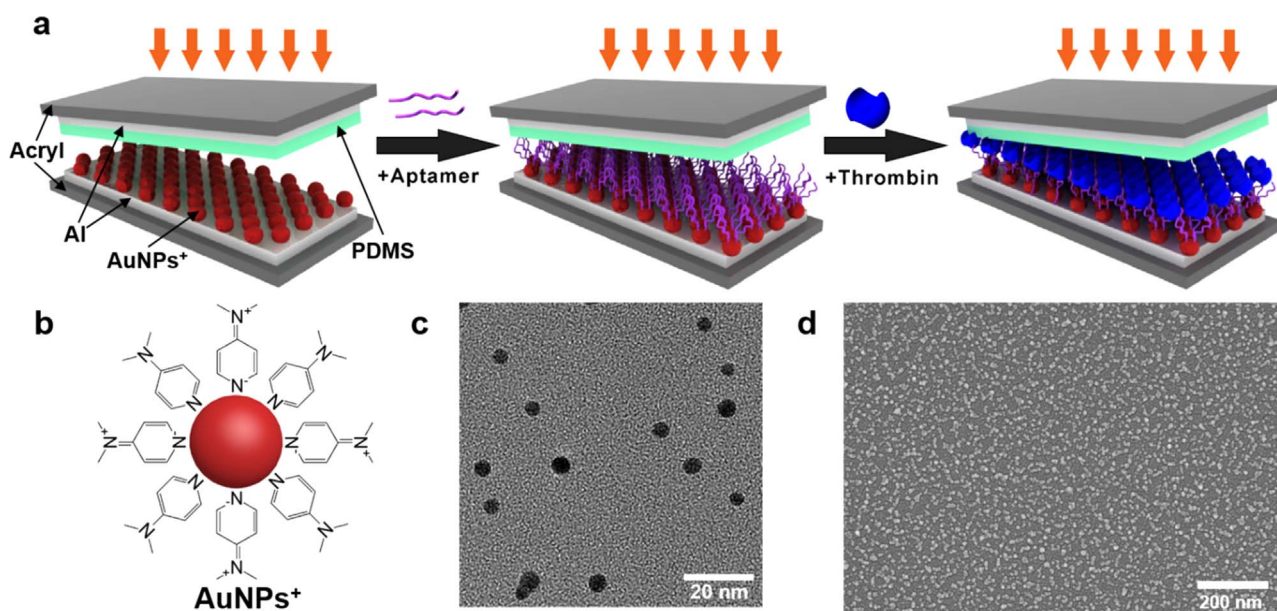


**Fig. 1.** (a) Schematic illustration of thrombin detection by triboelectric biosensors containing DNA aptamer-decorated Au NPs assembled onto the surface of Al film. (b) Positively charged Au NPs (Au NPs<sup>+</sup>) decorated with 4-(dimethylamino)pyridine (DMAP). (c) TEM image of Au NPs<sup>+</sup> and (d) SEM image of Au NPs<sup>+</sup> on Al film.

TENG biosensor.

### 2.3. Specific thrombin detection by TENG-based biosensor

To reduce disulfide bonds of thiol-modified synthetic oligonucleotides, 50  $\mu\text{L}$  of thrombin aptamers and random DNAs (100  $\mu\text{M}$ ) were incubated with 50  $\mu\text{L}$  of DL-dithiothreitol (DTT, 10 mM) for 30 min on a twister shaker (FinePCR TW3, Rose Scientific Ltd, Alberta, Canada) at ambient temperature. The reduced oligonucleotides were purified by removing DTT with Sephadex column (PD MiniTrap G-25, GE Healthcare, Sweden), followed by incubation with Au NP<sup>+</sup> (600 mg/L) for 30 min. Free oligonucleotides which were not attached to Au NP<sup>+</sup> were eliminated from oligonucleotide-modified Au NPs by using Amicon Ultra-15 centrifugal filter units (Millipore, Germany). After incubating 50  $\mu\text{L}$  of thrombin (50 nM), Str (100 nM), Lyso (100 nM) and a mixture of Str (100 nM) and Lyso (100 nM) in HEPES buffer (pH 7.26) with the as-prepared oligonucleotide-modified Au NPs for 30 min, free proteins were removed by using Amicon filter. The prepared Au NP<sup>+</sup>, oligonucleotide-modified Au NPs, and protein-treated oligonucleotide-Au NPs samples were dropped on Al substrate and dried for 2 h at room temperature. Additionally, to investigate whether thrombin in the clinical samples can be detected in our system, thrombin was introduced in 10% FBS followed by the same procedures to produce TENG biosensors. The data was compared to 10% FBS in the absence of thrombin.

### 2.4. Limit of detection (LOD) of the TENG aptasensor for thrombin

To verify the sensitivity of the TENG aptasensor for thrombin, 50  $\mu\text{L}$  of various concentrations of thrombin (0, 1, 2, 3, 4, 5, 10, 30, 50, 75 and 100 nM) in HEPES buffer were incubated with aptamer-modified Au NPs for 30 min. After removing free proteins by Amicon filter, output voltage and current of the TENG was measured. From the quantitative analysis, a calibration curve showing a relationship between the thrombin concentration and output performance was developed. The LOD was determined using the  $3s_b/m$  criterion, where  $s_b$  is the standard deviation of a negative control (blank) and  $m$  is the slope in the linear range [31].

## 3. Results and discussion

The fabrication process of triboelectric biosensors containing DNA aptamer-decorated Au NPs for the detection of thrombin is shown in Fig. 1. Acryl is selected as a supporting substrate due to its strength, good machinability and low cost. Additionally, PDMS is chosen because of its flat conformal surface, easy fabrication, and enhancement of the triboelectric charging. To improve the performance of TENG, 4-(dimethylamino)pyridine (DMAP)-modified Au NPs with a positive  $\zeta$ -potential (+35 mV; Au NPs<sup>+</sup>) at pH 7 and an average diameter of  $4.8 \pm 0.6$  nm are assembled onto the surface of Al film (Fig. 1a–c) [26]. The uniformly assembled Au NP<sup>+</sup>, as characterized by scanning electron microscope (SEM) (Fig. 1d), increases the contact area between a

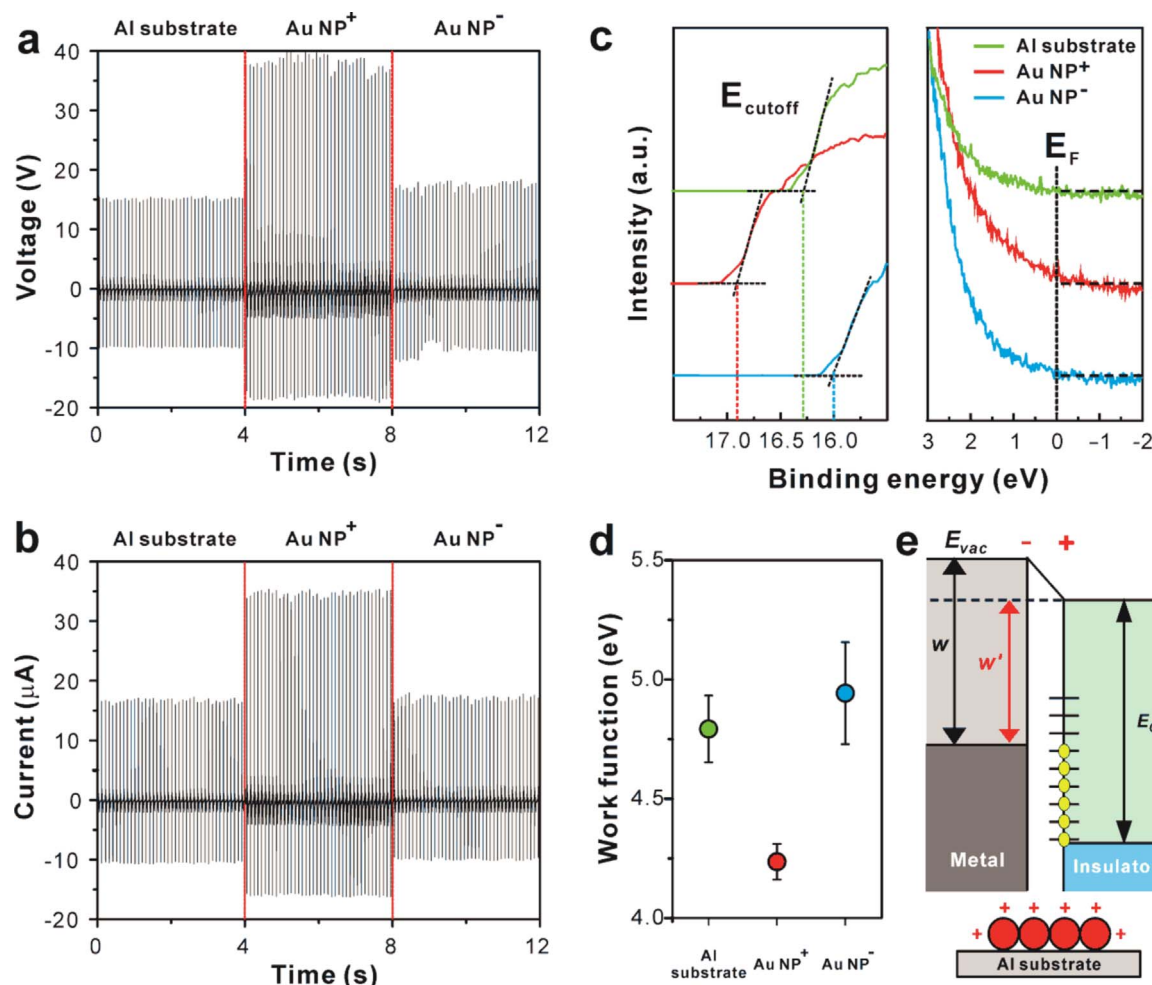


**Fig. 2.** (a, b) The output performance of Al-based TENGs with and without Au NP<sup>+</sup> or Au NP<sup>-</sup>. (c) UPS spectra and (d) work function of the reference Al layer, Au NP<sup>+</sup>-assembled and Au NP<sup>-</sup>-assembled TENG. (e) Energy band diagram of the Au NP<sup>+</sup>-assembled TENG. Yellow ovals and red circles indicate electrons and Au NPs, respectively.  $w$  and  $w'$  are work function and effective work function, respectively.

PDMS film as the top plate and an Al foil as the bottom plate as well as creates large potential drop, which drives the facile flow of electrons and increases the electrical output of the TENG. For the purpose of selective detection of thrombin, thiol-modified anti-thrombin aptamer is self-assembled onto the surface of Au NP<sup>+</sup> through strong Au-S interactions. Binding affinity of aptamers towards thrombin induces thrombin to selectively bind to the aptamer-decorated Au NP surface.

In general, the electrical signal generated in TENG can be explained by the triboelectric effects and electrostatic effects. To maximize the charge generation on both surfaces, the materials with the largest difference in the ability to attract electrons should be selected. Since the driving force for the triboelectrification process is basically the chemical potential difference between the two contact surfaces, the adsorption of certain molecules on the surface can influence the triboelectric charge density, and subsequently, the electrical output of the TENG. The Au NPs with opposite charges ( $\zeta$ -potentials of +35 mV and -24 mV) were tested to find the optimal conditions for the best performance of TENG. The TENG was mechanically triggered by a linear motor that provided dynamic impact with controlled force (50 N) at a frequency of 10 Hz.  $V_{oc}$  and  $I_{sc}$  were measured to characterize the generators' electric performance. After contact with negatively charged PDMS layer, the maximum output voltage and current of the reference Al substrate was up to 15 V and 17  $\mu$ A, respectively (Fig. 2a and b). The maximum peak value of positively charged Au NP<sup>+</sup>-assembled TENG reached 40 V and 36  $\mu$ A, respectively. In contrast, the maximum  $V_{oc}$  and  $I_{sc}$  of the TENG modified with carboxylic acid-modified Au NPs (Au NPs<sup>-</sup>, an average diameter of  $5.0 \pm 1.5$  nm, Fig. S3) were 17 V and 18  $\mu$ A, respectively [27–30]. From the output of voltage and current density, the assembled Au NP<sup>+</sup> onto the Al substrate is considered to transfer more surface charge, resulting in the enhancement in the electrical output performance [32].

Ultraviolet photoelectron spectroscopy (UPS) analysis was per-

formed to correlate the relationship between the work function and the surface property of the films (Fig. 2c). The work function ( $\Phi_s$ ) can be calculated from the threshold energy equation as  $\Phi_s = h\nu - |E_{cutoff} - E_F|$ , where  $h\nu$ ,  $E_{cutoff}$ , and  $E_F$  are the photon energy of the excitation light (UPS He source energy, 21.2 eV), the secondary electron cutoff energy and Fermi energy, respectively. The secondary electron cutoff energy was obtained using a linear tangent extension of the secondary electrons in the UPS spectrum. Fermi energy (0 eV) is calibrated by the Fermi level edge. Whereas the work function ( $\Phi_s$ ) of the reference Al and Au NP<sup>-</sup>-assembled TENG have  $4.79 \pm 0.14$  eV and  $4.94 \pm 0.21$  eV, respectively, the Au NP<sup>+</sup>-assembled TENG was shown to have the smallest work function of  $4.24 \pm 0.08$  eV (Fig. 2d).

Based on these results, we illustrated energy band diagram of the TENG without and with Au NP<sup>+</sup> or Au NP<sup>-</sup> (Figs. 2e and S4). Compared with Al substrate, the exterior surface of Au NPs<sup>+</sup> carrying a nucleophile such as DMAP has a positive charge and excess electron is migrated to the interior of the Au NPs. This induces a permanent dipole at the Au NP<sup>+</sup> interface, which up-shifts the vacuum level ( $E_{vac}$ ) by introducing a dipole-induced potential step at the interface, thus, down-shifts the effective metal work function ( $w'$ ) (Fig. 2e) [32–36]. Whereas an interfacial dipole of Au NP<sup>-</sup>, in which a permanent dipole is oriented toward the inner surface of Au NPs, down-shifts the vacuum level, resulting in an increase in the effective metal work function and subsequent decrease in the difference of surface potential with the Fermi energy of the insulator (Fig. S4). The surface charges may also affect the electrostatic effects because the dipole can induce the additional dipole moment inside the PDMS. However, it is negligible because the electrons through the external circuit flow to maintain the electrostatic equilibrium state by the electrostatic induction. The thickness of the Au NPs and biomolecules are also too thin (~nm).

The highly selective recognition of thrombin by TENG biosensor can be achieved by the use of anti-thrombin aptamer. The anti-

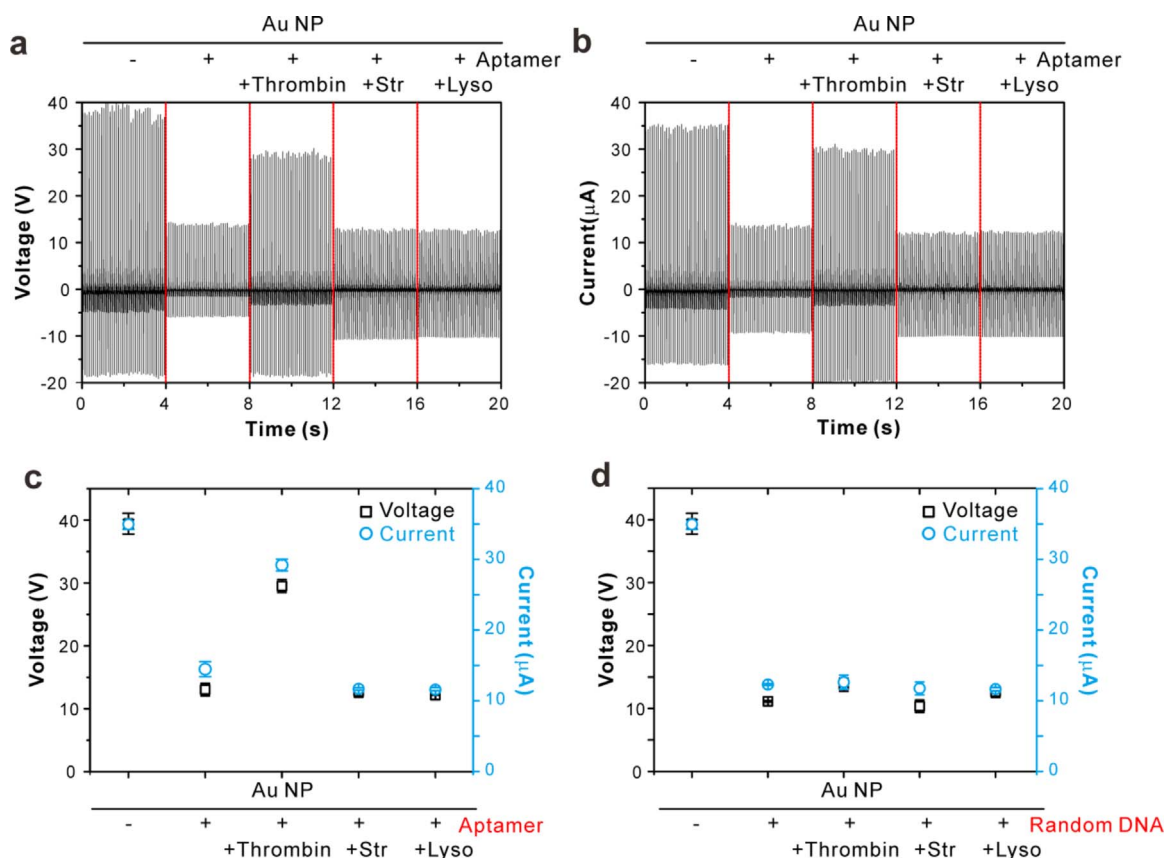


**Fig. 3.** (a) Output voltage and (b) current of the Au NP<sup>+</sup>-assembled TENG after anti-thrombin aptamer decoration and subsequent addition of various proteins. (c) Selectivity of anti-thrombin aptamer-decorated TENG biosensor for the detection of thrombin. (d) The output signals of random DNA-decorated TENG after addition of proteins.

thrombin 29-mer aptamer binds to one of the two anion binding sites, heparin-binding exosite of thrombin with a high affinity ( $K_d=0.5$  nM) and forms a stable intramolecular G-quadruplex structure [9–11]. To demonstrate the specificity of aptamers for recognition of thrombin, random DNA was used as a negative control. Furthermore, Str and Lyso with positive  $\zeta$ -potentials (+13.0 mV and +2.0 mV, respectively) were used as nonspecific proteins. The reference Al substrate showed the average output voltage and current density of  $15 \pm 0.09$  V and  $17 \pm 0.4$   $\mu$ A, respectively. Upon treatment with Au NPs<sup>+</sup>, the average output performance was increased to  $39 \pm 1.7$  V and  $35 \pm 0.8$   $\mu$ A. Interestingly, after the modification of anti-thrombin aptamers on the assembled Au NPs<sup>+</sup> in TENG, the average output was decreased to  $13 \pm 0.5$  V and  $15 \pm 1.0$   $\mu$ A due to negatively charged phosphate backbone of aptamers. As the aptamer-conjugated TENG biosensor was incubated with target protein thrombin ( $\zeta$ -potential of  $-0.57$  mV), it was clearly seen that the electrical signals were considerably enhanced to  $27 \pm 0.9$  V and  $29 \pm 0.7$   $\mu$ A in the  $V_{oc}$  and  $I_{sc}$ , respectively. However, incubation with single non-specific protein such as Str and Lyso as well as with a mixture of Str and Lyso did not induce any noticeable change in output performance ( $13 \pm 0.2$  V and  $12 \pm 0.2$   $\mu$ A in Str-treated TENG,  $12 \pm 0.1$  V and  $12 \pm 0.2$   $\mu$ A in Lyso-treated TENG, and  $11 \pm 0.8$  V and  $11 \pm 0.8$   $\mu$ A in Str and Lyso-treated TENG, respectively) (Figs. 3a–c and S5), suggesting a key role of specific recognition between aptamer and thrombin.

The change in the electrical output can be explained by the surface potential changed by introducing the functional groups on the Au NPs. The anti-thrombin 29-mer aptamer composed of a quadruplex “core” sequence and additional base-pairing sequence binds to heparin-binding site of thrombin by duplex structure of hairpin conformation [9–11]. The binding of the negatively charged aptamer results in the orientation of the dipoles toward the Au NPs, increasing the effective metal work function. Upon interaction with thrombin, however, the outer surface of the TENG possesses a relatively positive charge compared to the aptamer-conjugated TENG due to the physical block of negatively charged phosphate backbone of aptamers by the thrombin, decreasing the metal work function. This change in the surface potential upon binding with the thrombin will increase the electrostatic potential between the Au NPs and PDMS, thereby, the output performance of the TENG, as proved in Figs. 2 and S4.

The electrostatic potentials generated in the Au NP<sup>+</sup>-assembled TENG after aptamer decoration and subsequent addition of thrombin were also calculated by the COMSOL multi-physics software. The material parameters of the Al and PDMS, taken from the COMSOL simulation software, are used for the finite element analysis. The dielectric constant of Au and PDMS are 6.9 and 3 respectively. We assumed that the electric potential ( $U_{bottom}$ ) of the surface of aptamer-decorated Au NP<sup>+</sup> layer is zero in fully released TENG. The surface potential of top PDMS layer ( $U_{top}$ ) could be expressed by  $U_{top}=\sigma d_{gap}/\epsilon_0$ , where  $\sigma$  is the triboelectric charge density,  $\epsilon_0$  is the vacuum permittivity of free space ( $8.85 \times 10^{-12}$  F/m). The gap distance ( $d_{gap}$ ) between Au NP<sup>+</sup> and PDMS was assumed to be approximately 0.1 mm. It is clearly seen that the decoration of anti-thrombin aptamer on the Au NP<sup>+</sup>-assembled TENG decreases the difference in electrostatic potentials. The calculated surface charge density ( $\sigma$ ) on the surfaces of top PDMS layer also decreased from  $7.1$   $\mu$ C/m<sup>2</sup> to  $2.13$   $\mu$ C/m<sup>2</sup> by the decoration. This may be explained in terms of the surface potential, in which the work function is expected to be increased by the formation of – charges on the Au NPs, as understood in Fig. 2. Upon incubation with target protein thrombin, surface potentials are recovered, comparable to that of the Au NP<sup>+</sup>-assembled TENG (Fig. S6).

Moreover, it is of note that the random DNA-conjugated TENG samples showed similar output signals of  $11 \pm 0.4$  V and  $12 \pm 0.3$   $\mu$ A to those of aptamer-conjugated TENG. Even after reaction with proteins including thrombin, Str and Lyso, the random DNA-conjugated TENG samples did not display any alteration of voltage and current density ( $10$ – $14$  V and  $12$ – $13$   $\mu$ A, respectively, Figs. 3d and S7). Furthermore, we also extended the approach to detect thrombin in the clinical

samples. For this purpose, we prepared the thrombin in 10% fetal bovine serum (FBS) containing the rich variety of proteins [37] and conducted the identical procedures to produce TENG biosensors. As shown in Fig. S8, the thrombin in the complex media also produced significantly enhanced electrical signals ( $30 \pm 1.3$  V and  $29 \pm 1.5$   $\mu$ A), similar to the purified thrombin sample while the FBS samples without thrombin displayed a negligible output performance ( $14 \pm 0.5$  V and  $14 \pm 0.4$   $\mu$ A). For practical applications, the influence of salt was also examined for the interaction between proteins and Au NPs<sup>+</sup>. The TENG biosensors reacted with thrombin generated similar output currents regardless of salt concentrations tested (1.0 mM and 1.0 M of NaCl) (Fig. S9). Taken together, the TENG aptasensor is highly selective toward thrombin detection.

To observe morphological changes, SEM and atomic force microscope (AFM) images of the Al film coated with aptamer-conjugated Au NPs before and after incubation with proteins were obtained (Fig. S10). The aptamer-conjugated Au NPs-assembled Al film showed monodisperse and well-distributed spherical particles. After addition of thrombin, the SEM image of the aptamer-conjugated TENG surface was faint and poor, presumably due to the binding of thrombin to its aptamer. However, the addition of negative control proteins such as Str and Lyso to the aptamer-conjugated TENG did not cause any structural transition compared with the aptamer-conjugated TENG.

In order to confirm that thrombin is attached to the aptamer-conjugated TENG biosensor, AFM analysis was further carried out. The aptamer-conjugated Au NPs-assembled film displayed a regular and even surface. Upon the incubation with thrombin whose size is about 4 nm [38,39], the surface became relatively rough with an appearance of characteristic peaks. In contrast, Str- and Lyso-treated Au NPs films showed similar surface to that of the aptamer-conjugated Au NPs film. Surface root-mean-square roughness ( $R_{rms}$ ) values (averaged over  $1 \times 1$   $\mu$ m<sup>2</sup>) of aptamer-conjugated Au NPs films, thrombin-treated, Str-treated, and Lyso-treated Au NPs films were determined to be 1.23, 1.79, 1.39, and 1.22 nm, respectively. From the structural characterization, it was confirmed that the aptamer-conjugated TENG sensor specifically interacts with thrombin.

A sensor's sensitivity is greatly influenced by the type of transducer such as electrochemical, mass, optical and thermal detection methods [2]. Thus, ultrasensitivity offers the TENG to act as an excellent analytical tool for monitoring target molecules of interest [40]. To determine the sensitivity of our assay, limit of detection (LOD) tests were conducted [31]. As shown in Figs. 4a and S11, the output signals increased upon increasing the concentration of thrombin ( $R^2=0.99$ ), and we obtained a LOD of 0.41 nM at an S/N of 3. It should be highlighted that this LOD is as sensitive as those of previously reported [1–3,10–17], even without the need for any external equipment. The high sensitivity of our triboelectric aptasensor is attributable to the TENG structure which has the Au NP<sup>+</sup> with the large difference in work function and large surface area. The electricity generated by the interactions with thrombin directly lit up from 6 to 17 green LEDs depending on thrombin concentration (Fig. 4b) without the use of external source of electricity, which showed great potential as a future promising simple detection systems as well as facilitating label-free sensing without complex labelling of expensive dyes.

#### 4. Conclusions

In summary, a triboelectric biosensor based on contact electrification has been developed for highly selective, label-free and self-powered detection of thrombin using aptamers as a recognition element. Our approach offers a number of achievements in using TENG for biosensors. To maximize the output performance of TENG, the Au NPs<sup>+</sup> with the smallest work function and large surface area are selected and used to produce the TENG. They are considered to transfer more surface charge, caused by a decrease in the effective metal work function and subsequent increase in the difference of

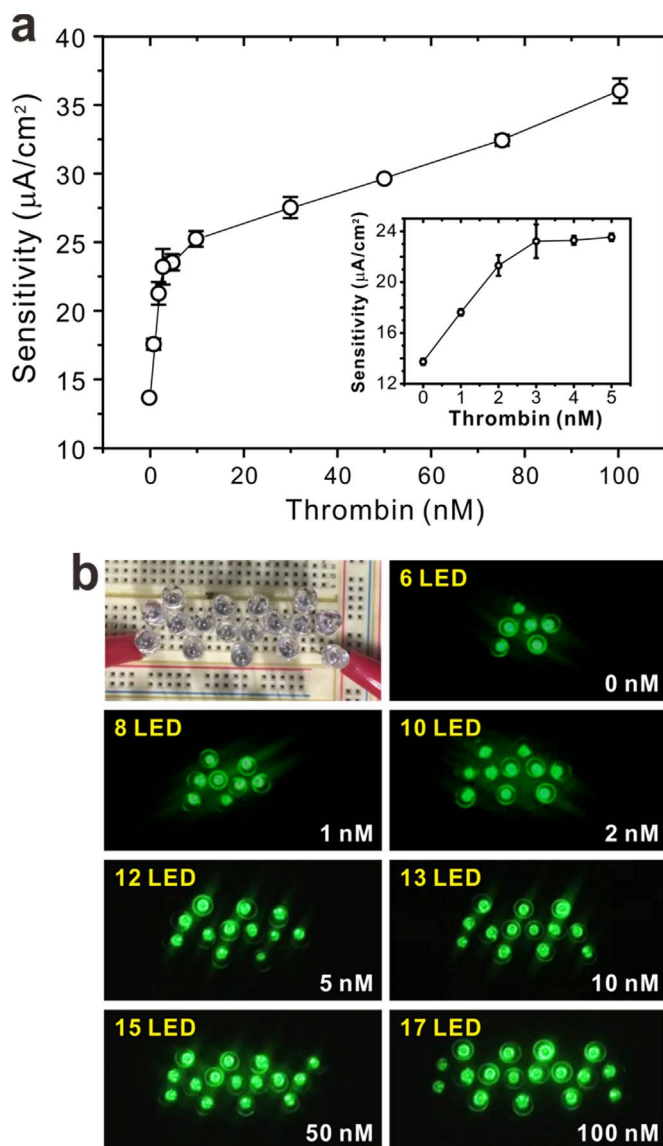


**Fig. 4.** (a) Detection sensitivity of anti-thrombin aptamer-decorated TENG biosensors depending on thrombin concentration. Inset graph shows the sensitivity after addition of thrombin in the low nanomolar range. (b) Photograph of the lighted LED lamp after interaction with various concentrations of thrombin.

surface potential with the Fermi energy of the insulator. As a recognition element, the use of aptamers offers triboelectric biosensor high selectivity toward thrombin, even in clinical samples. To demonstrate the specificity of aptamers for recognition of thrombin, random DNA as well as nonspecific proteins including Str and Lyso were used as negative controls. Furthermore, the triboelectric biosensor achieves high detection sensitivity, which is directly demonstrated by the number of LED lights even without the use of external source of electricity and complex labelling of expensive dyes. Due to its selectivity, simple fabrication, low cost, label-free and convenient monitoring mechanism, the self-powered triboelectric biosensor could be used to detect any type of biomolecules by changing biological recognition elements for portable biomedical diagnosis and environmental monitoring in the near future.

### Acknowledgements

Dr. Y. K. Jung and K. N. Nam contributed equally to this work. This work was supported by the National Research Foundation of Korea (NRF) grant funded by the Korea government (NRF-

2015R1A1A3A04001437 and 2010-0028684).

### Appendix A. Supporting information

Supplementary data associated with this article can be found in the online version at doi:10.1016/j.nanoen.2016.09.039.

### References

- [1] Y. Wang, L. Bao, Z. Liu, D.-W. Pang, *Anal. Chem.* 83 (2011) 8130–8137.
- [2] B. Leca-Bouvier, L.J. Blum, *Anal. Lett.* 38 (2005) 1491–1517.
- [3] J.-I. Hahm, *Sensors* 11 (2011) 3327–3355.
- [4] J. Hu, P.-C. Zheng, J.-H. Jiang, G.-L. Shen, R.-Q. Yu, G.-K. Liu, *Anal. Chem.* 81 (2009) 87–93.
- [5] C.A. Holland, A.T. Henry, H.C. Whinna, F.C. Church, *FEBS Lett.* 484 (2000) 87–91.
- [6] M.L. Nierodzik, S. Karpatkin, *Cancer Cell* 10 (2006) 355–362.
- [7] M.A. Shuman, P.W. Majerus, *J. Clin. Invest.* 58 (1976) 1249–1258.
- [8] S.D. Jayasena, *Clin. Chem.* 45 (1999) 1628–1650.
- [9] D.M. Tasset, M.F. Kubik, W. Steiner, *J. Mol. Biol.* 272 (1997) 688–698.
- [10] B. Deng, Y. Lin, C. Wang, F. Li, Z. Wang, H. Zhang, X.-F. Li, X.C. Le, *Anal. Chim. Acta* 837 (2014) 1–15.
- [11] P.-H. Lin, R.-H. Chen, C.-H. Lee, Y. Chang, C.-S. Chen, W.-Y. Chen, *Colloid Surf. B* 88 (2011) 552–558.
- [12] B. Strehlitz, N. Nikolaus, R. Stoltenburg, *Sensors* 8 (2008) 4296–4307.
- [13] Y.K. Jung, T.W. Kim, H.G. Park, H.T. Soh, *Adv. Funct. Mater.* 20 (2010) 3092–3097.
- [14] W.U. Dittmer, A. Reuter, F.C. Simmel, *Angew. Chem. Int. Ed.* 43 (2004) 3550–3553.
- [15] H. Chang, L. Tang, Y. Wang, J. Jiang, J. Li, *Anal. Chem.* 82 (2010) 2341–2346.
- [16] Y.K. Jung, T. Lee, E. Shin, B.-S. Kim, *Sci. Rep.* 3 (2013) 3367.
- [17] J.J. Li, X. Fang, S.M. Schuster, W. Tan, *Angew. Chem. Int. Ed.* 39 (2000) 1049–1052.
- [18] Z.-H.G. Zhu Lin, Y.S. Zhou, Y. Yang, P. Bai, J. Chen, Z.L. Wang, *Angew. Chem.* 125 (2013) 5169–5173.
- [19] H. Zhang, Y. Yang, T.-C. Hou, Y. Su, C. Hu, Z.L. Wang, *Nano Energy* 2 (2013) 1019–1024.
- [20] Z.L. Wang, J. Chen, L. Lin, *Energy Environ. Sci.* 8 (2015) 2250–2282.
- [21] J. Zhong, Q. Zhong, Q. Hu, N. Wu, W. Li, B. Wang, B. Hu, J. Zhou, *Adv. Funct. Mater.* 25 (2015) 1798–1803.
- [22] J. Zhong, Y. Zhang, Q. Zhong, Q. Hu, B. Hu, Z.L. Wang, J. Zhou, *ACS Nano* 8 (2014) 6273–6280.
- [23] Q. Zhong, J. Zhong, B. Hu, Q. Hu, J. Zhou, Z.L. Wang, *Energy Environ. Sci.* 6 (2013) 1779–1784.
- [24] L.S. McCarty, G.M. Whitesides, *Angew. Chem. Int. Ed.* 47 (2008) 2188–2207.
- [25] F.-R. Fan, L. Lin, G. Zhu, W. Wu, R. Zhang, Z.L. Wang, *Nano Lett.* 12 (2012) 3109–3114.
- [26] Y. Choi, M. Gu, J. Park, H.-K. Song, B.-S. Kim, *Adv. Energy Mater.* 2 (2012) 1510–1518.
- [27] M. Brust, M. Walker, D. Bethell, D.J. Schiffrin, R. Whyman, *J. Chem. Soc. Chem. Commun.* 7 (1994) 801–802.
- [28] A.C. Templeton, W.P. Wuelfing, R.W. Murray, *Acc. Chem. Res.* 33 (2000) 27–36.
- [29] A. Wijaya, K. Hamad-Schifferli, *Langmuir* 24 (2008) 9966–9969.
- [30] R.R. Arvizo, O.R. Miranda, M.A. Thompson, C.M. Pabelick, R. Bhattacharya, J.D. Robertson, V.M. Rotello, Y.S. Prakash, P. Mukherjee, *Nano Lett.* 10 (2010) 2543–2548.
- [31] Y.K. Jung, J. Kim, R.A. Mathies, *Anal. Chem.* 87 (2015) 3165–3170.
- [32] K.N. Kim, Y.K. Jung, J. Chun, B.U. Ye, M. Gu, E. Seo, S. Kim, S.-W. Kim, B.-S. Kim, J.M. Baik, *Nano Energy* 26 (2016) 360–370.
- [33] M. Obradovic, M.D. Vece, D. Grandjean, K. Houben, P. Lievens, *J. Phys. Condens. Matter* 28 (2016) 035303.
- [34] Y. Zhang, O. Pluchery, L. Caillard, A.-F. Lamic-Humblot, S. Casale, Y.J. Chabal, M. Salmeron, *Nano Lett.* 15 (2015) 51–55.
- [35] M.D. Scanlon, P. Pelijo, M.A. Méndez, E. Smirnov, H.H. Girault, *Chem. Sci.* 6 (2015) 2705–2720.
- [36] S. Braun, W.R. Salaneck, M. Fahlman, *Adv. Mater.* 21 (2009) 1450–1472.
- [37] X. Zheng, H. Baker, W.S. Hancock, F. Fawaz, M. McCaman, E. Pungor Jr., *Biotechnol. Prog.* 22 (2006) 1294–1300.
- [38] S. Rinker, Y. Ke, Y. Liu, R. Chhabra, H. Yan, *Nat. Nanotechnol.* 3 (2008) 418–422.
- [39] X. Ma, P. Shrotriya, *Mechanics of Biological Systems and Materials* 4, Springer International Publishing, Switzerland, 2014, pp. 163–168 Ch. 23.
- [40] R.P. Singh, *Int. J. Electrochem.* 2011 (2011) 125487.



**Dr. Yun Kyung Jung** is an Assistant Professor of School of Biomedical Engineering at Inje University, Korea. She received her Ph.D. from Department of Chemical and Biomolecular Engineering, Korea Advanced Institute of Science and Technology (KAIST). Her recent research interest is focused on polydiacetylene-based biosensor, anti-cancer drug delivery using carbon nanodots, cell imaging probe and triboelectric biosensor for self-powered in-field analysis.



**Dr. Jeong Min Baik** is now an Associate Professor in School of Materials Science and Engineering, Ulsan National Institute of Science and Technology (UNIST). He received his Ph.D. from Pohang University in Department of Materials Science and Engineering in 2006. His recent research interest is focused on the synthesis of nanomaterials and nanostructures such as nanoparticles, nanowires, nanolayers and nanopores for the applications of Energy-Conversion Devices and Nanophotonic Devices. Particular interests are concerned with the development of Piezoelectric/Triboelectric Nanogenerators and Artificial Photosynthesis.



**Kyeong Nam Kim** is a Ph.D. candidate under the supervision of Prof. Jeong Min Baik at School of Materials Science and Engineering, Ulsan National Institute of Science and Technology (UNIST). His master's research focuses on development of composite and textile structure based piezoelectric generators/triboelectric generators for sustainable energy conversions, biocompatible device, and fundamental study.



**Dr. Byeong-Su Kim** is an Associate Professor of Department of Chemistry at the Ulsan National Institute of Science and Technology (UNIST), Korea. He received Ph.D. in chemistry at University of Minnesota in 2007. After postdoctoral researches at MIT for two years, he started his independent career at UNIST since August 2009. His research and education programs cover a broad span of macromolecular chemistry in the study of novel polymer and hybrid nanomaterials, including the molecular design and synthesis of self-assembled polymers, layer-by-layer assembly for functional thin films, and now expand to complex macromolecular systems such as carbon nanomaterials.